December 2003

The *Drosophila* Selenoprotein BthD Is Required for Survival and Has a Role in Salivary Gland Development

So Yeon Kwon
National Institutes of Health, Bethesda, Maryland

Paul Badenhorst
National Institutes of Health, Bethesda, Maryland

F. Javier Martin-Romero
National Institutes of Health, Bethesda, Maryland

Bradley A. Carlson
National Institutes of Health, Bethesda, Maryland

Bruce M. Paterson
National Institutes of Health, Bethesda, Maryland

See next page for additional authors

MOLECULAR AND CELLULAR BIOLOGY, Dec. 2003, p. 8495–8504 Vol. 23, No. 23
0270-7306/03/$08.00+0 DOI: 10.1128/MCB.23.23.8495–8504.2003

The *Drosophila* Selenoprotein BthD Is Required for Survival and Has a Role in Salivary Gland Development

So Yeon Kwon,[1,2] Paul Badenhorst,[3] F. Javier Martin-Romero,[1]† Bradley A. Carlson,[1] Bruce M. Paterson,[4] Vadim N. Gladyshev,[5] Byeong Jae Lee,[2]* and Dolph L. Hatfield[1]*

Basic Research Laboratory,[1] Laboratory of Molecular Cell Biology,[3] and Laboratory of Biochemistry,[4] Center for Cancer Research, National Cancer Institute, National Institutes of Health, Bethesda, Maryland 20892; Department of Biochemistry, University of Nebraska, Lincoln, Nebraska 68588[5]; and Laboratory of Molecular Genetics, School of Biological Sciences, Seoul National University, Seoul 151-742, Korea[2]

Received 31 March 2003/Returned for modification 9 May 2003/Accepted 21 August 2003

Selenium is implicated in many diseases, including cancer, but its function at the molecular level is poorly understood. BthD is one of three selenoproteins recently identified in *Drosophila*. To elucidate the function of BthD and the role of selenoproteins in cellular metabolism and health, we analyzed the developmental expression profile of this protein and used inducible RNA interference (RNAi) to ablate function. We find that BthD is dynamically expressed during *Drosophila* development. *bthD* mRNA and protein are abundant in the ovaries of female flies and are deposited into the developing oocyte. Maternally contributed protein and RNA persist during early embryonic development but decay by the onset of gastrulation. At later stages of embryogenesis, BthD is expressed highly in the developing salivary gland. We generated transgenic fly lines carrying an inducible gene-silencing construct, in which an inverted *bthD* genomic-cDNA hybrid is under the control of the *Drosophila* Gal4 upstream activation sequence system. Duplex RNAi induced from this construct targeted BthD mRNA for destruction and reduced BthD protein levels. We found that loss of BthD compromised salivary gland morphogenesis and reduced animal viability.

Selenium is an important micronutrient in the diet of many life forms, including vertebrates (reviewed in reference 16), *Drosophila* (28), and the lower plant *Chlamydomonas reinhardtii* (33). Selenium has been said to be a cancer chemopreventive agent, to prevent heart disease and other cardiovascular and muscle disorders, to inhibit viral expression, to delay the progression of AIDS in human immunodeficiency virus-positive patients, to slow the aging process, and to have roles in immune function, mammalian development, and male reproduction (see reviews in reference 15).

During protein synthesis, selenium is incorporated into nascent selenopeptides as the amino acid selenocysteine (Sec) (16). Sec is specified by the codon UGA that normally terminates protein synthesis. However, in selenium-containing proteins, a specialized stem-loop structure located in the mRNA (designated the Sec insertion sequence [SECIS] element) (27) stipulates UGA in the open reading frame to incorporate Sec.

The identification and characterization of selenoproteins are essential to understanding the role of this class of proteins in development and in cellular metabolism. Computer programs designed to find SECIS elements in expressed sequence tags and genomic DNA have been developed as a means of identifying selenoprotein genes (22, 23). Such in silico searches for SECIS elements have identified three selenoprotein genes in the *Drosophila* genome (8, 28). One of the selenoproteins is selenophosphate synthetase 2 (SPS2), a 43-kDa protein that is involved in the biosynthesis of Sec through the generation of selenophosphate, the selenium donor compound. SPS2 in *Drosophila* has previously been described (17) and is the homolog of a protein previously found in mammals (12, 21, 26). In addition to SPS2, two novel proteins were found (8, 28): a 28-kDa protein designated BthD and a 12-kDa, glycine-rich protein designated G-rich (28). Since SPS2 is involved in Sec biosynthesis, BthD and G-rich should be responsible for the biological effects of selenium in fruit flies. However, the specific functions of these proteins are not known.

RNA interference (RNAi), which is also called posttranscriptional gene silencing, has proven to be a powerful tool for disrupting gene expression. This technique was initially developed in plants (3, 10) and nematodes (9) and more recently in *Drosophila* (19, 20, 32), zebra fish (24), and mice (6, 13, 14). RNAi can be used to interfere with gene expression both transiently (by introducing double-stranded RNA [dsRNA] directly into cells) and stably (by inserting an appropriate construct that produces the targeting dsRNA into the genome). The advantage of using inheritable or inducible RNAi is that the phenomenon becomes a permanent feature of an organism, and the effect can often be triggered under a variety of different conditions and/or at different times of development.

We have characterized the expression profile of BthD and find that it is expressed dynamically during *Drosophila* development. BthD is abundant in the developing ovary of female flies, and large amounts of RNA and protein are deposited into the early embryo. At the later stages of development, BthD

* Corresponding author. Mailing address for B. J. Lee: Laboratory of Molecular Genetics, School of Biological Sciences, Seoul National University, Seoul 151-742, Korea. Phone: 82-2-880-6775. Fax: 82-2-872-9019. E-mail: imbglmg@plaza.snu.ac.kr. Mailing address for D. L. Hatfield: National Cancer Institute, National Institutes of Health, Building 37, Room 2D09, Bethesda, MD 20892. Phone: (301) 496-2797. Fax: (301) 435-4957. E-mail: hatfield@dc37a.nci.nih.gov.

† Present address: Departmento de Bioquimica y Biologia Molecular, Facultat de Ciencias, Universidad de Extremadura, 06071 Badajoz, Spain.

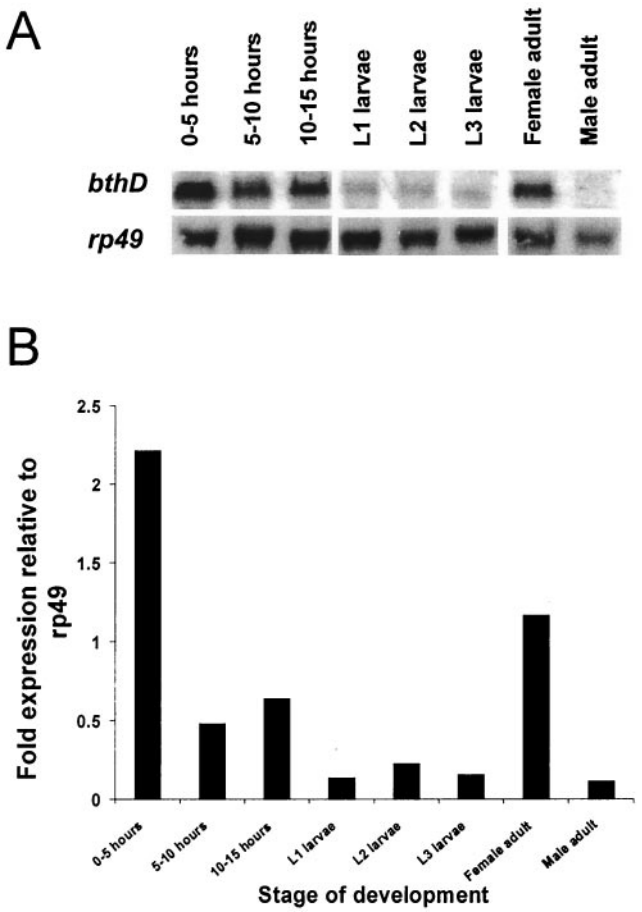

FIG. 1. Expression of *bthD* mRNA. (A) Northern blot analysis. Total RNA was extracted from adults and staged embryo and larval collections and was hybridized with probes specific to *bthD* mRNA or *rp49* as shown. (B) mRNA quantization. *bthD* mRNA levels were normalized (using a PhosphorImager) to *rp49* as a control and plotted as shown.

expression reinitiates in the developing salivary gland. The subcellular distribution of BthD at these stages suggests that BthD might have roles in protein secretion or processing. To address this, we have used inducible RNAi to ablate BthD expression. Transgenic lines that express dsRNA as an extended hairpin loop (19) were generated and used to interfere specifically with BthD expression. We find that BthD is required for viability and normal salivary gland morphogenesis.

MATERIALS AND METHODS

Northern analysis. Total RNA was isolated from staged embryos, larvae, and adult flies according to the protocol of Montell et al. (29). A total of 30 μg of total RNA from each stage was fractionated on a 2.2 M formaldehyde–1.2% agarose gel and transferred to a nylon membrane. Probes for hybridization were labeled using Ready-To-Go DNA labeling beads (Amersham), and hybridization was performed at 68°C in Quickhyb hybridization solution (Stratagene). To allow reprobing of the membrane, bound probe was removed by washing the blot with boiling 0.1% sodium dodecyl sulfate. Removal of the probe was confirmed before the next hybridization. A PCR-amplified fragment of full-length *bhtD* cDNA was used as a probe, and *rp49* was used as a loading control.

Antibody production. To allow expression of BthD in *Escherichia coli*, full-length *bthD* cDNA was mutated to convert the Sec-encoding TGA codon to TGC (Cys codon). Mutagenesis was performed using a PCR-directed mutagenesis strategy (18) and the following primer sets: 5′-GGAATTCCATATGCCAC CAAAACGGAACA-3′, 5′-ACGACGAAAGACTCGGCAGGATCGGCAGT GCTC-3′, 5′-GAGCACTGCCGATCCTGCCGAGTCTTTCGTCGT-3′, and 5′-CCGCTCGAGTTAGGCATGATGATGATGATGATGCCTCCTCCGCTT GGCACCG-3′ (the underlined characters designate the mutation sites). The altered cDNA was cloned into pET-15b (Novagen) to generate a six-histidine-tagged fusion derivative of BthD. The His-tagged BthD fusion protein was overexpressed in *E. coli* strain BL21(DE3)/pLysS. The fusion protein was purified employing Qiagen Ni-nitrilotriacetic acid (NTA) beads and used to immunize rabbits (Spring Valley, Woodbine, Md.).

Denaturing and nondenaturing gel electrophoresis. *Drosophila* SL2 cells were harvested and resuspended in phosphate-buffered saline (PBS) containing protease inhibitor cocktail (Sigma). Cells were lysed by sonication on ice, and 10 μg of total protein was electrophoresed on Novex Tris-glycine–10% polyacrylamide gels (Invitrogen) under either denaturing or nondenaturing conditions (as described in the manufacturer's instructions).

Cell culture and transfection. *Drosophila* SL2 cells (Invitrogen) were maintained in HyQ CCM-3 medium (HyClone) containing 50 U of penicillin and streptomycin (Gibco/BRL). SL2 cells were plated in six-well plates and transfected using Lipofectin (Invitrogen). In each transfection, 10 μg of *bthD* dsRNA was used. At 72 h after the transfection, cells were harvested and used for Western blotting.

Genetics and *Drosophila* strains. Flies were raised at 25°C. *daGal4* (39) or *fkhGal4* (31) was used to drive ubiquitous or salivary gland-specific expression, respectively. The enhancer trap line NT33 (35) was used as a marker for the embryonic salivary gland.

Inducible RNAi construct. For the *bthD* RNAi construct, genomic and cDNA fragments were amplified using PCR with primers containing unique restriction sites. The genomic fragment was isolated by PCR as an *Eco*RI-to-*Bgl*II fragment and cloned into pUAST (5). The inverted cDNA sequence digested with *Kpn*I and *Xba*I was ligated sequentially to the genomic fragment-containing vector. Ligated RNAi constructs were transformed into DH5α cells (Invitrogen). Primer sequences for RNAi constructs were as follows: *bthD* genomic forward, 5′-CCGGAATTCATGCCACCAAAACGGAACAA-3′; *bthD* genomic reverse, 5′-GGAAGATCTGAAGTTGGTGCCTTCGTTTTCCTGTGCTTCC-3′; *bthD* cDNA forward, 5′-CGGGGTACCCCTCGTTTTCCTGTGCTTCC-3′; and *bthD* cDNA reverse, 5′-CTAGTCTAGAATGCCACCAAAAACGGAACAA-3′. The construct was transformed into w^{1118} flies by P-element-mediated transformation (36). Adult G_0 transformants were identified by outcrossing to w^{1118} and balanced over SM5 or TM3 balancer chromosomes. Four different homozygous, viable *UAS-BthDRNAi* lines were used in all experiments. No reduction in viability or morphological abnormalities was observed in any of the upstream activation sequence (UAS) lines in the absence of a GAL4 driver.

Western blot analysis. Cells and embryos were lysed in PBS buffer containing a complete protease mix (Roche). Anti-BthD antisera were used at a 1:2,000 dilution for Western analysis. Antitubulin antibody (Developmental Studies Hybridoma Bank) was used as a control at a 1:1,000 dilution. Each antigen was detected using an enhanced chemiluminescence Western blotting detection kit (Amersham Bioscience).

Immunohistochemistry and immunofluorescence. Embryo fixation and immunohistochemistry were performed as described previously (2). Immunoassaying of ovaries was performed as described previously (25). For immunofluorescence, fluorescein isothiocyanate- and Cy3-conjugated anti-immunoglobulin G secondary antibodies (Jackson ImmunoResearch) were used. Samples were mounted in Vectashield (Vector Laboratories) and viewed using a confocal microscope (Bio-Rad model MRC 1024). For immunohistochemistry, biotinylated anti-immunoglobulin G secondary antibodies and a Vectastain ABC kit (Vector Laboratories) were used. Antibodies were used at the following dilutions: for mouse anti-β-galactosidase (anti-β-Gal) (Promega), 1:10,000, and for rabbit anti-BthD, 1:200 (immunofluorescence) or 1:1,000 (immunocytochemistry). DNA was stained using SYTOX Green (Molecular Probes). Embryos were staged as given previously (7).

Salivary glands, imaginal disks, and the gut and trachea were dissected from third-instar larvae and incubated in fixative (PBS, 3.7% formaldehyde, 0.1% Triton X-100) for 20 min on ice. After extensive washes in PBS, samples were mounted in Vectashield containing DAPI (4′,6′diamidino-2-phenylindole) (Vector Laboratories). To visualize the actin cytoskeleton, dissected third-instar salivary glands were incubated in 37% formaldehyde for 4 min, washed extensively with PBT (PBS, 0.1% Triton X-100), and then incubated overnight in PBS containing 0.1% Triton X-100, 10% fetal calf serum, and 0.8 U of rhodamine-phalloidin (Molecular Probes)/ml. After four washes in PBT, samples were mounted in Vectashield.

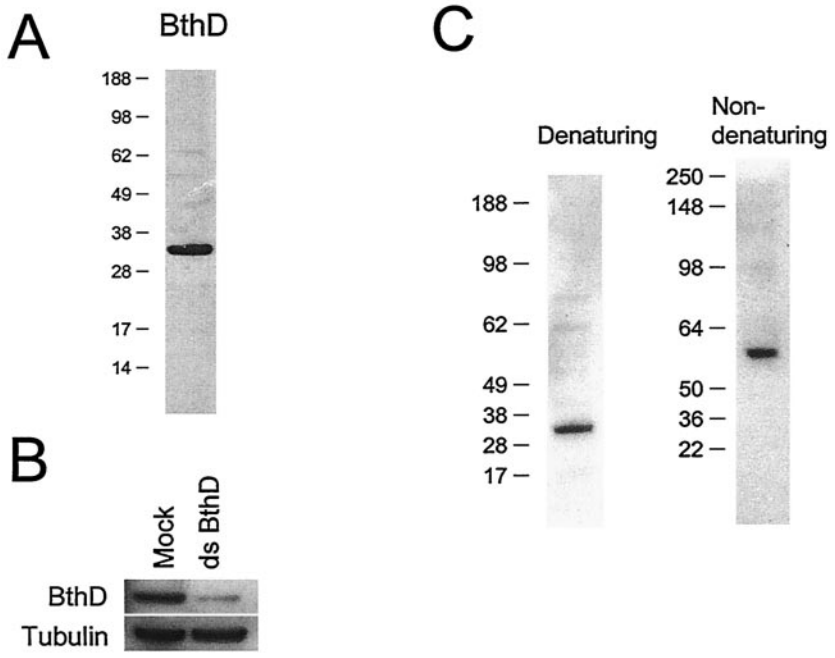

FIG. 2. Antibody detection of BthD in SL2 cells. (A) Western blot analysis in extracts. (B) Western blot analysis in RNAi-treated cells. SL2 cells were treated with *bthD* dsRNA, and an extract was prepared and compared (using gel electrophoresis) to an extract from untreated cells as shown. (C) Western blot analysis of denaturing and nondenaturing gels. SL2 cell extracts were electrophoresed on polyacrylamide gels as shown.

RESULTS

BthD RNA and protein distribution. The expression of BthD during development and in adult flies was first examined by Northern blotting. Total RNA was isolated from adult male and female flies and from staged collections of embryos and larvae that spanned development. As shown in Fig. 1A, *bthD* mRNA appeared to be expressed at high levels during early embryogenesis (0-5 hours lane) and in adult females (Female adult lane) and at moderate levels in mid- and late-phase embryogenesis (5-10 hours lane and 10-15 hours lane, respectively). *bthD* mRNA was poorly expressed in the larval stages (L1 larvae, L2 larvae, and L3 larvae lanes) and in adult males (Male adult lane). Quantitation of *bthD* mRNA levels relative to those of *rp49* (used as a loading control) confirmed these observations, as shown in Fig. 1B.

We also observed the expression of BthD in adult female, but not male, flies by ^{75}Se labeling (28). To visualize selenoproteins, adult flies were maintained overnight on ^{75}Se-containing medium (28) to allow incorporation into nascent polypeptides. Three selenoproteins, BthD, SPS2, and G-rich, which had previously been observed by using ^{75}Se labeling in *Drosophila* (28), were observed in adult females, but only BthD was not detected in males (data not shown).

As a tool to characterize the expression of BthD in more detail, we generated specific antibodies against the recombinant protein. The resultant antisera specifically detected one band in extracts from SL2 cells (Fig. 2A). This band had the expected molecular weight of BthD (see denaturing gel in Fig. 2A) and comigrated with the protein labeled by ^{75}Se (data not shown). To further confirm the specificity of anti-BthD antibody, we treated SL2 cells with dsRNA directed against BthD (Fig. 2B). The abundance of BthD was markedly decreased relative to that of untreated, control cells. Tubulin was used as a gel loading control. Interestingly, when BthD was run on a nondenaturing gel it migrated as a larger protein (Fig. 2C), suggesting that it might occur as a dimer.

Anti-BthD antibodies were used to examine protein expression in ovaries of adult female flies. Ovaries were dissected from adult flies, and BthD was visualized by confocal microscopy (Fig. 3). BthD, which is shown in red in Fig. 3A, is abundantly expressed in ovarioles from the earliest stages (see upper-left portion of the panel) until the completion of oocyte development (see right-hand portion of the panel). The results of higher magnification of stage 8 of the developing oocyte suggest that BthD occurs in the cytoplasm (Fig. 3D). To visualize nuclei, DNA was labeled with Sytox Green dye, as shown by the green staining in Fig. 3B and E. Simultaneous visualization of BthD and DNA revealed that the protein is found exclusively in the cytoplasm of the developing oocyte and not in nurse cell nuclei or in the nuclei of the surrounding follicle cells, as shown in Fig. 3C and F.

Embryonic expression profile of BthD. We examined BthD protein distribution in embryos. Consistent with the high levels of expression of BthD protein and RNA in the ovary of adult female flies, antibody staining using anti-BthD antibodies revealed that BthD is expressed ubiquitously, and at high levels, in the early embryo (Fig. 4A; a syncytial blastoderm stage 2 embryo is shown). The abundance of maternally contributed BthD declined after cellularization of the blastoderm (stage 4) and was much reduced by the onset of germband retraction (stage 10). At later stages of development, BthD expression appeared to initiate in the salivary gland. BthD was first de-

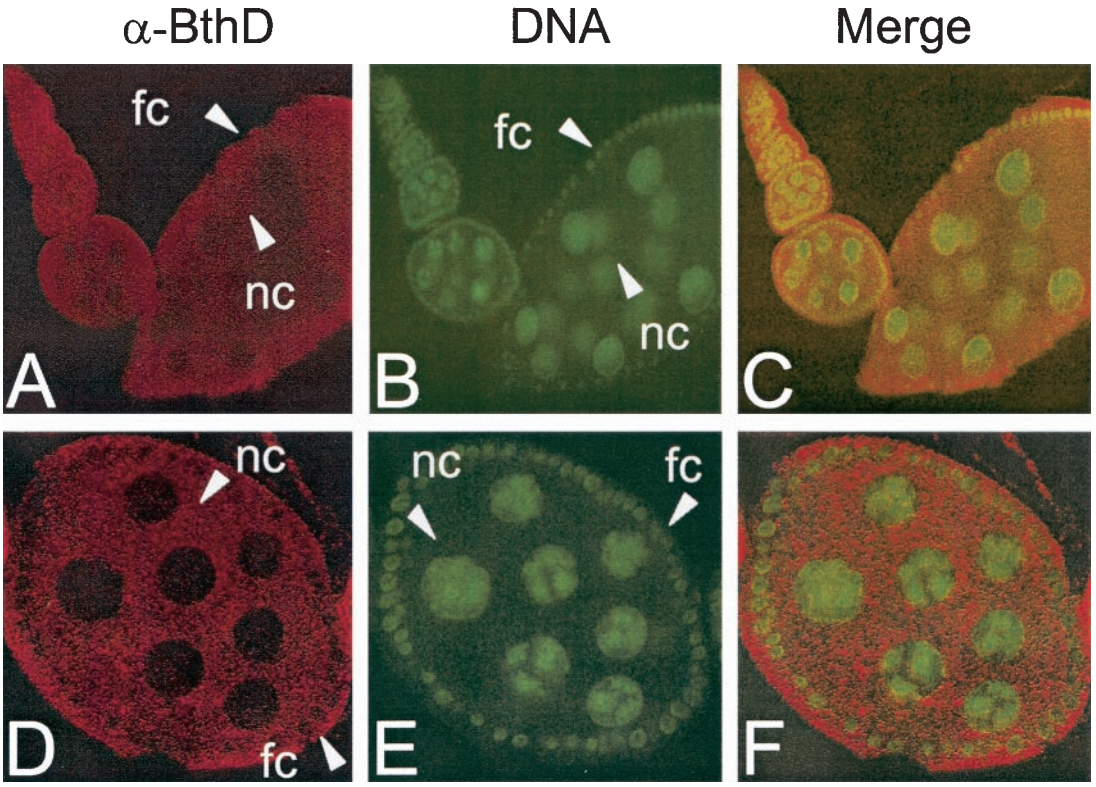

FIG. 3. Localization of BthD in developing egg chambers. BthD antibodies (α-BthD) and DNA dye were used (as described in Materials and Methods) to visualize BthD expression (shown in red) (A and D) and DNA (shown in green) (B and E). (C and F) Merged images. (D to F) Higher-magnification images of the stage 8 egg chamber show that BthD is expressed throughout the cytoplasm of the follicle (fc) and nurse cells (nc). Magnification for panels A to C is ×100 and for panels D to F is ×200.

tected at stage 14, and this accumulation was fully apparent by stages 15 and 16.

Salivary gland expression of BthD was confirmed by comparing BthD distribution to that of Pasilla, a known salivary gland marker (35). As shown in Fig. 4B, double-label immunofluorescence (using antibodies against β-Gal [shown in red] and BthD [shown in green]) of *pasilla*-enhancer trap line N33 embryos confirmed that BthD is expressed in the salivary gland. BthD expression, however, initiated relatively late in salivary gland development. Although robust Pasilla expression was observed in stage 12 embryos, BthD was absent. BthD expression was apparent at stage 14. Higher-magnification images of these embryos (see panels labeled "Salivary gland" in Fig. 4B) reveal that BthD expression was primarily cytoplasmic. At stage 14, significant staining was noted in the lumen of the salivary gland. By stage 15, lumenal staining was decreased, although BthD staining was still observable in the cytoplasm of the cells that flanked the lumen.

Subcellular distribution of BthD. We analyzed in greater detail the subcellular distribution of BthD in the early embryo and the salivary gland. Interestingly, subcellular distribution of BthD was quite dynamic. At the earliest stages, the majority of BthD was distributed in large sphere-like structures (Fig. 5A). These were located in the cortical cytoplasm, just beneath the cell membrane, at the extreme periphery of the embryo (see inset in Fig. 5A). As embryonic development proceeded and the cortical cytoplasm expanded, the major accumulation of BthD tracked the cortical cytoplasm into the interior of the embryo. At this stage, large accumulations of BthD appeared to break down and were absorbed into punctate granules that encircled regions once occupied by spheres.

This particulate distribution was also seen in salivary glands (Fig. 5B). The majority of BthD was located in punctate granules that surrounded the nuclei in salivary gland cells. This was seen in both stage 14 and stage 16 embryos. In stage 14 embryos, high BthD staining was also detected in the lumen of the salivary gland. By stage 16, lumenal staining was much reduced. We attempted to use known markers for subcellular compartments for identification of these granules. Staining of SL2 cells with anti-BthD antibodies recapitulated the punctate staining profile. Costaining with NBD-C6-ceramide, which marks the Golgi apparatus, indicated that BthD staining overlaps the Golgi (Fig. 5C).

Inducible RNAi targets BthD. We used an inducible RNAi strategy to ablate BthD function. Our approach is summarized in Fig. 6A. A construct was synthesized in which an inverted *bthD* genomic-cDNA hybrid was placed under the control of the GAL4-UAS. Expression from this construct led to the synthesis of a hybrid RNA which, after splicing of the two introns from the genomic sequence, snapped back to form a dsRNA. This construct was transformed into flies, and four independent transgenic lines were recovered. All lines showed equivalent results.

Induction of the *bthD* dsRNA synthesis was able to reduce

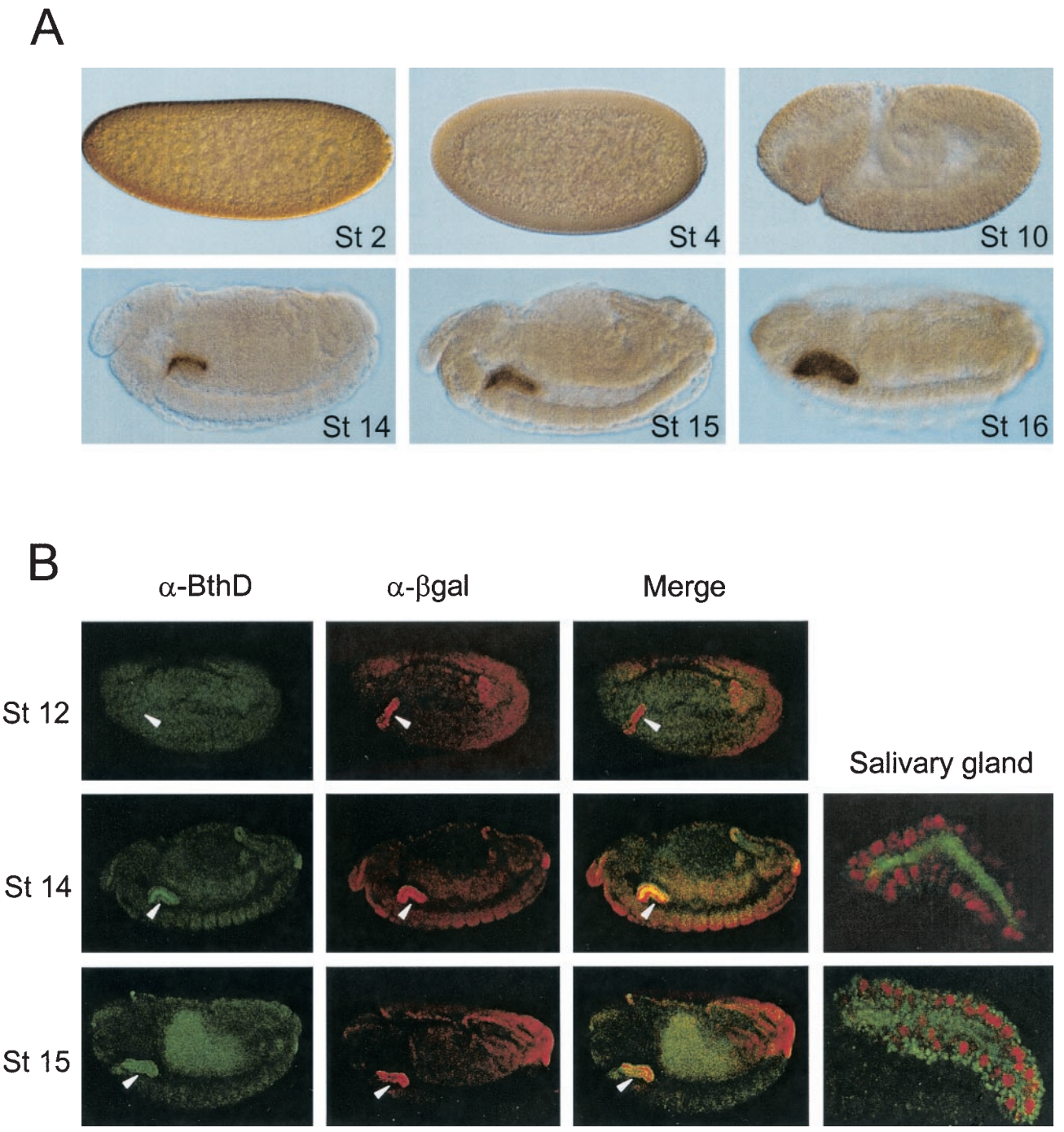

FIG. 4. BthD embryonic expression profile. (A) Expression during embryogenesis. Embryos were stained with anti-BthD antibodies, and BthD expression was revealed using horseradish peroxidase-coupled secondary antibodies. Magnification is ×100. (B) Salivary gland-specific expression. Embryos containing the *pasilla*-enhancer trap (NT33), which expresses β-Gal under the control of the *pasilla* promoter, were stained with antibodies against β-Gal (α-βgal) (red) and BthD (α-BthD) (green). Magnification of embryos is ×100. Higher-magnification (×630) images of the salivary glands from stage (St) 14 and stage 15 embryos are also shown alongside the merged embryo images. In all panels, embryos are oriented with the anterior side to the left and the dorsal side up.

BthD protein levels. As shown in Fig. 6B, overexpression (using the salivary gland-specific *fkhGAL4* driver) of the UAS-RNAi construct decreased BthD protein levels in late-stage-16 embryos. The *daGAL4* driver was also used to direct ubiquitous expression of the UAS-RNAi construct. *daGAL4*-mediated expression also reduced *bthD* mRNA and protein levels (data not shown).

BthD is required for survival and specifically for salivary gland morphogenesis. We next examined how ablation of BthD affects survival and viability. Induction using either *da-*

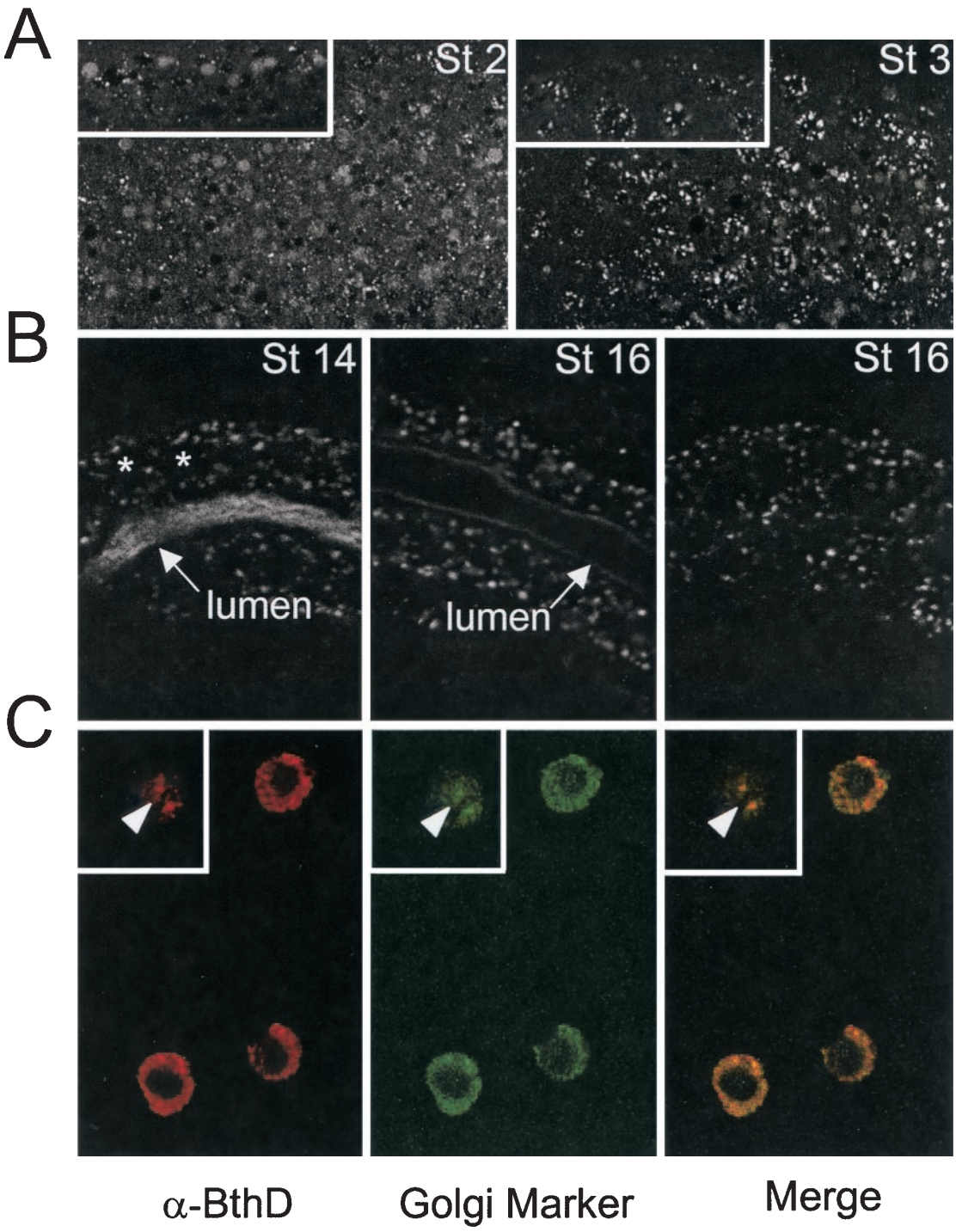

FIG. 5. BthD subcellular distribution. (A) High-magnification (×1,260) confocal images of BthD protein distribution in syncytial embryos (stages [St] 2 and 3). Insets are confocal sections revealing the cortical cytoplasm (immediately below the membrane). (B) BthD distribution in the salivary gland. BthD is localized to granules that encircle the nuclei of the salivary gland cells (asterisks signify nuclei that were stained with DAPI [data not shown]). Punctate BthD staining can be seen in confocal sections that traverse the lumen of the salivary gland or traverse the exterior of the gland. The lumen of the salivary gland is indicated by arrows. (C) Distribution in SL2 cells. SL2 cells were stained with anti-BthD antibodies (red) and NBD-C6-ceramide (green), which reveals the Golgi apparatus. Insets show a top view of stained cells, and arrows indicate colocalization of BthD and the Golgi marker.

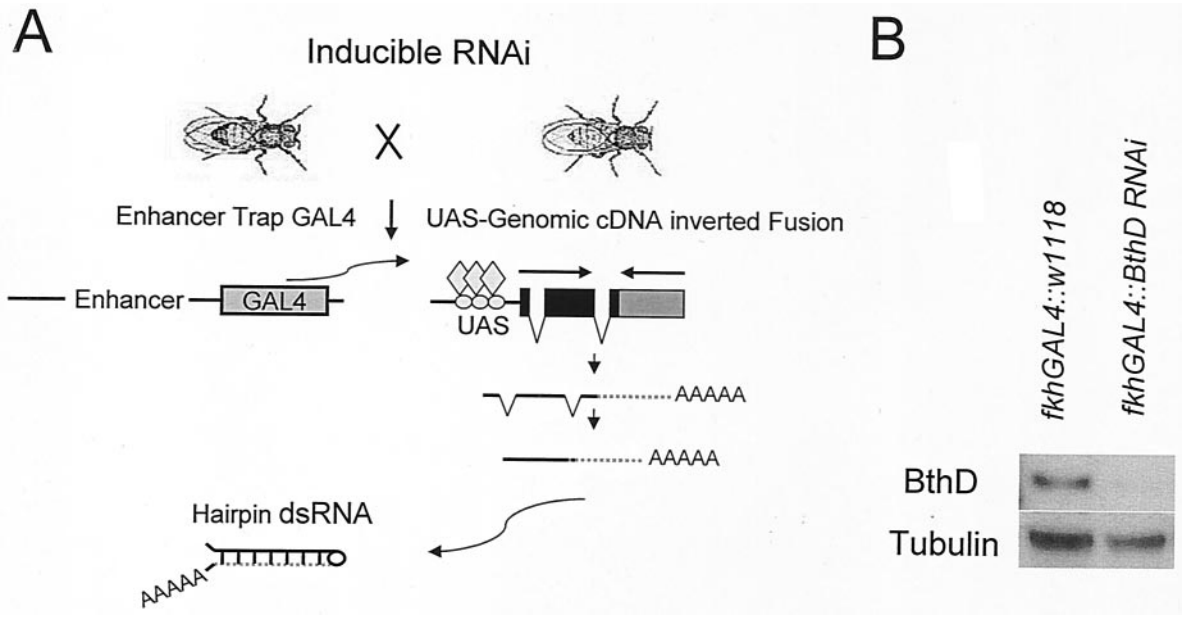

FIG. 6. BthD ablation using inducible RNAi. (A) Strategy for inducible dsRNA synthesis. (B) Induction of dsRNA using the salivary gland-specific *fkhGAL4* driver. Extracts from stage 16 *fkhGAL4*/+ or *fkhGAL4*/*UAS-BthDRNAi* embryos were analyzed by Western blotting using anti-BthD antibodies and antitubulin antibodies as a loading control.

GAL4 or *fkhGAL4* did not significantly affect embryo survival. However, the number of adult flies that were recovered was significantly reduced. We collected defined numbers of first-instar larvae and assayed survival by counting the number of adult flies to eclose. As shown in Fig. 7A, both *daGAL4*- and *fkhGAL4*-mediated dsRNA induction reduced the number of adult flies that were recovered from approximately 100 to 21.5 and 28, respectively. Larval survival was not significantly affected, but most animals died shortly after pupariation (Fig. 7B).

As we had shown that BthD is expressed in the embryonic salivary gland, we examined whether RNAi induction affected salivary gland development. The salivary gland is an interesting model organ system, as salivary gland cells are set aside during embryonic stages and the final cell number for each gland is established by the completion of embryogenesis. During larval life, the cell number does not increase and growth is mediated only by an increase in cell size.

Induction of *bthD* RNAi either (using *fkhGAL4*) specifically in the salivary gland or (using *daGAL4*) throughout the entire embryo had profound effects on larval salivary gland morphogenesis. Total cell number was not decreased, as the same number of nuclei was still detected by DAPI staining of third-instar larval salivary glands (Fig. 8). However, cell size was dramatically reduced. Glands were significantly smaller, and nuclei were more closely packed. This is clearly seen in the insets to Fig. 8B and C. The effects of *bthD* RNAi appear to be specific to the salivary gland. Although the *daGAL4* driver directed expression throughout the embryo from early stages of development, no significant effects on embryo development, or on the development of other larval tissues, were noted. For example, no differences in imaginal disk morphology were seen between *daGal4*/+ and *daGal4*/*UAS-BthdRNAi* larvae (Fig. 8D and E). In addition, no differences were seen in the size or morphology of the third-instar larval gut between *daGal4*/+ and *daGal4*/*UAS-BthdRNAi* larvae (Fig. 8F and G) or in the developing trachea of these fly lines (data not shown).

The reduction in salivary gland size was confirmed by staining with rhodamine-phalloidin to visualize cortical actin. The size of individual cells was dramatically reduced in *daGal4*/*UAS-BthdRNAi* salivary glands (data not shown). Although in vivo generation of *bthD* dsRNA had a profound effect on larval salivary gland morphology, staining with antibodies against the embryonic salivary gland marker Pasilla (35) showed little or no effect on embryonic salivary gland development (data not shown). This observation is consistent with the expression of BthD late in embryonic development and suggests that BthD does not have a function in the early embryonic phases of salivary gland development.

DISCUSSION

BthD is one of three selenoproteins identified in *Drosophila* (8, 28). As part of a program to understand the role of selenoproteins in health and development, we examined the biological function of BthD. Homologs of this protein are present in a variety of organisms, including humans, but none of the members of this family have been previously characterized. Our analysis shows that BthD is expressed dynamically during *Drosophila* development. High levels are detected in the adult ovary, and a large maternal dowry of BthD protein and RNA is contributed to early embryos. At late stages of embryogenesis, BthD accumulates in the developing salivary gland. Using an inducible RNAi system, we ablated BthD expression in the salivary gland and found that BthD is required for proper salivary gland morphogenesis. Loss of BthD reduces animal viability.

We had anticipated that the BthD expression profile would

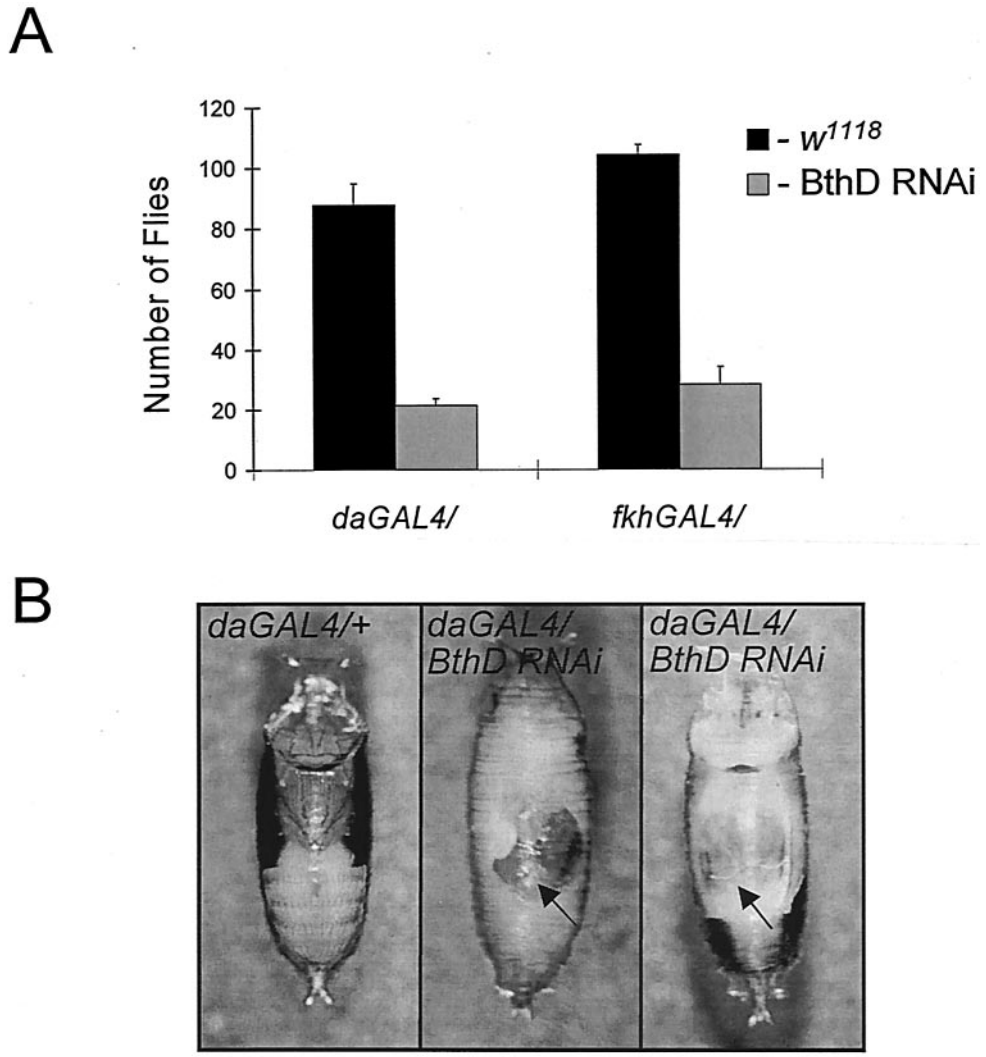

FIG. 7. Viability and pupae phenotypes in BthD-deficient organisms. (A) Viability after induction of *bthD* dsRNA. Homozygous *daGAL4* or *fkhGAL4* virgin female flies were crossed to either w^{1118} or *UAS-BthDRNAi* males. Progeny first-instar larvae were collected and placed in vials (150 each). The number of adult flies of each genotype that eclosed was recorded. Data are the means and standard deviations of five independent determinations. (B) *daGAL4*/+ and *daGAL4*/*UAS-BthDRNAi* pupae.

provide important clues to function. To a certain extent this expectation was realized. The most noticeable feature of BthD expression is its relatively dynamic nature. Both RNA and protein abundance and distribution fluctuate considerably. Such an expression profile argues against BthD having a general function in cellular metabolism. This is in marked contrast to the other two *Drosophila* selenoproteins, SPS2 and G-rich. Analyses using antibodies against either SPS2 or G-rich indicate that these proteins are expressed ubiquitously and constantly throughout development (unpublished data). While the actions of G-rich are unclear, the functions of SPS2 are well established. SPS2 underpins Sec biosynthesis, as it catalyzes the synthesis of selenophosphate for its donation to the acceptor intermediate in Sec biosynthesis (12, 21, 26), and it also indirectly serves in *Drosophila* as an antioxidant (30).

In tissues where it is expressed, BthD is localized in the cytoplasm and is not detected in the nucleus. BthD staining in SL2 cells colocalizes with that of a known Golgi marker. It is tempting to speculate, therefore, that BthD protein traffics through the Golgi to another compartment. The gross expression profile of BthD suggests that BthD has some function in protein secretion or processing. Both regions where BthD is most highly expressed correspond to high biosynthetic activity. In the developing egg chambers, nurse cells abutting the developing oocyte synthesize large quantities of protein that drive the early postfertilization development of the *Drosophila* embryo. The salivary glands synthesize digestive enzymes and pupal glue proteins (4).

In early embryos, the cytoplasmic distribution of BthD is dynamic. At the earliest stages that we examined, the majority of BthD was found in large spherical structures. These are located immediately below the plasma membrane in the cortical cytoplasm and do not correspond to the known distributions of yolk particles or lipid vesicles (38). As development

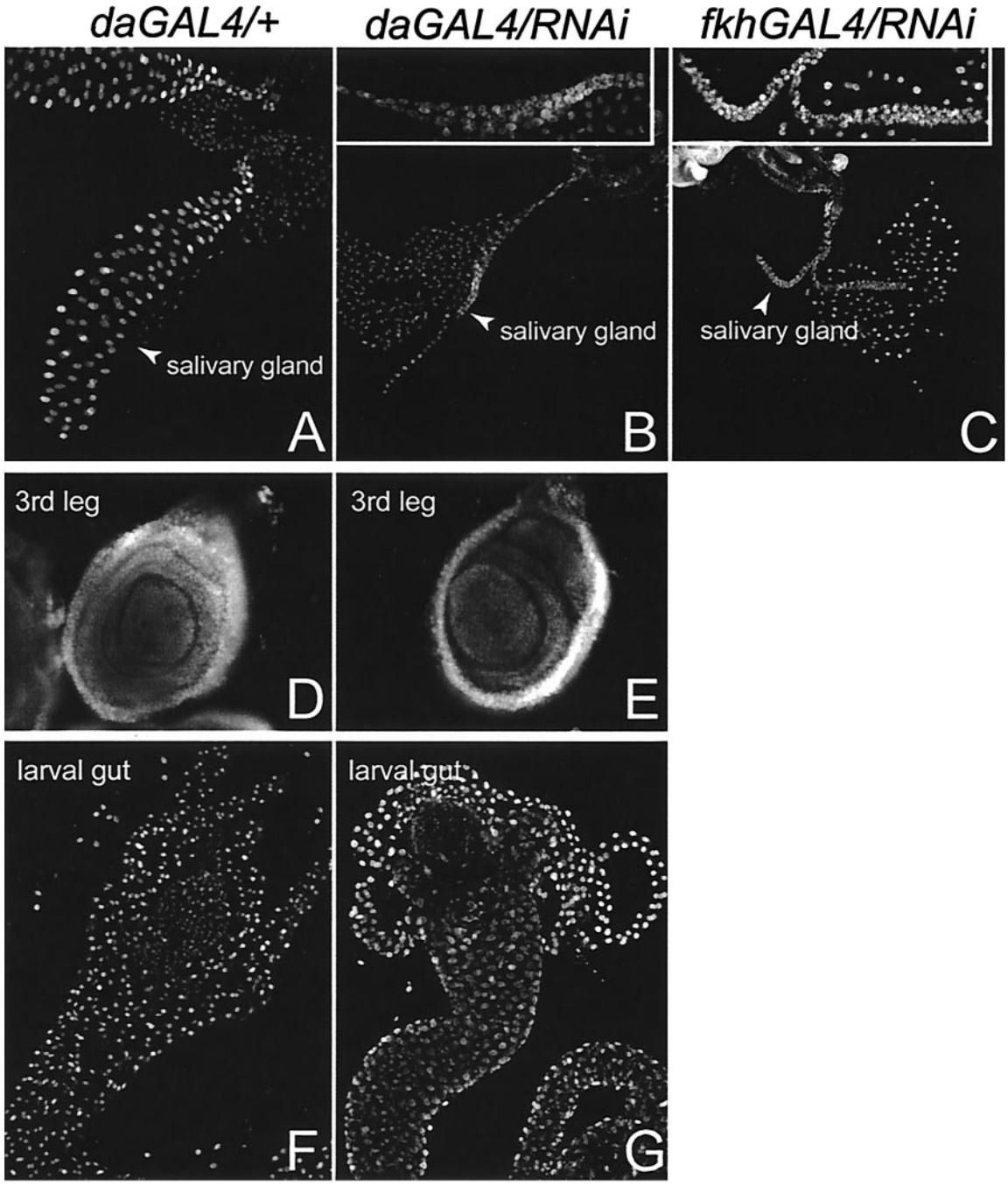

FIG. 8. Salivary gland morphogenesis. Salivary glands were dissected from third-instar *daGAL4*/+ (A), *daGAL4*/*UAS-BthDRNAi* (B), and *fkhGAL4*/*UAS-BthDRNAi* (C) larvae, fixed, and stained with DAPI to visualize nuclei (×50 magnification). The insets in panels B and C show images of *daGAL4*/*UAS-BthDRNAi* and *fkhGAL4*/*UAS-BthDRNAi* salivary glands, respectively, at higher magnification (×100). As controls, leg imaginal disks from third-instar *daGAL4*/+ (D) and *daGAL4*/*UAS-BthDRNAi* (E) larvae were dissected, fixed, and stained with DAPI (×100 magnification) and the gut from third-instar *daGAL4*/+ (F) and *daGAL4*/*UAS-BthDRNAi* (G) larvae was fixed and stained with DAPI (×50 magnification).

proceeds these structures appear to break down or be absorbed into small vesicles or particles. In the salivary gland, this particulate staining is recapitulated. It is also interesting that when BthD can first be detected in the salivary gland, high levels are seen in the lumen. At later stages, lumenal staining is decreased. It is possible that decreased lumenal staining corresponds with gland activity. Salivary glands are believed to be functional and to actively secrete by larval hatching (1).

We used an inducible RNAi strategy to selectively remove BthD expression and elucidate its function in salivary glands. Inducible RNAi has been successfully employed to target gene function in *Drosophila* (11, 19, 32, 37). Analysis using two-color

fluorescent-protein imaging indicates that the effects of RNAi are cell autonomous.

We used two GAL4 drivers to induce RNAi expression: *daGAL4*, which drives ubiquitous expression from early embryonic stages (39), and *fkhGAL4*, which drives salivary gland-specific expression (31). We were able to reduce BthD levels in late-stage embryos and observed similar phenotypes with both drivers. Quantitative reverse transcription-PCR showed that *bthD* mRNA levels were also reduced (data not shown). Ubiquitous expression of *bthD* dsRNA did not have general effects on cell viability and morphology. The major effect we observed was on salivary gland morphogenesis. Removal of BthD caused a dramatic reduction in the size of the third-instar larval salivary gland. Cell number was not decreased. However, cell size was greatly affected.

We were unable to address the functions of BthD in ovary or early embryo development, as our constructs were based on pUAST, which does not express well in the female germ line (34). Moreover, the *daGAL4* driver initiates expression after early embryonic BthD levels have started to decline. The elucidation of the expression of BthD and its effect on salivary gland morphogenesis in *Drosophila*, however, appears to suggest a novel role for selenoproteins in development. It will be of considerable interest to elucidate the specific role of BthD action in salivary gland morphogenesis and survival.

ACKNOWLEDGMENTS

We express our sincere appreciation to D. Andrew, JHMI, for the ET ps(N33) *Drosophila* line and the Pasilla antibody and to Susan H. Garfield, CCR Confocal Microscopy Core, LEC, NCI, NIH, for her expert assistance with confocal microscopy.

This work was supported in part by NIH GM061603 (V.N.G.), 21C Frontier Functional Human Genome Project from the Ministry of Science and Technology of Korea (B.J.L.), and the Wellcome Trust (P.B.).

REFERENCES

1. **Andrew, D. J., K. D. Henderson, and P. Seshaiah.** 2000. Salivary gland development in *Drosophila melanogaster*. Mech. Dev. **92:**5–17.
2. **Badenhorst, P.** 2001. Tramtrack controls glial number and identity in the *Drosophila* embryonic CNS. Development **128:**4093–4101.
3. **Bernstein, H. E., A. M. Denli, and G. J. Hannon.** 2001. The rest is silence. RNA **7:**1509–1521.
4. **Bradley, P. L., A. S. Haberman, and D. J. Andrew.** 2001. Organ formation in *Drosophila*: specification and morphogenesis of the salivary gland. Bioessays **23:**901–911.
5. **Brand, A. H., and N. Perrimon.** 1993. Targeted disruption of gene function in *Drosophila* by RNA interference (RNA-i): a role for nautilus in embryonic somatic muscle formation. Development **118:**401–415.
6. **Brummelkamp, T. R., R. Bernards, and R. Agami.** 2002. A system for stable expression of short interfering RNAs in mammalian cells. Science **296:**50–553.
7. **Campos-Ortega, J. A., and V. Hartenstein.** 1985. The embryonic development of *Drosophila melanogaster*. Springer-Verlag, Berlin, Germany.
8. **Castellano, S., N. Morozova, M. Morey, M. J. Berry, F. Serras, M. Corominas, and R. Guigo.** 2001. In silico identification of novel selenoproteins in the *Drosophila melanogaster* genome. EMBO Rep. **2:**97–702.
9. **Fire, A., S. Xu, M. K. Montgomery, S. A. Kostas, S. E. Driver, and C. C. Mello.** 1998. Potent and specific genetic interference by double-stranded RNA in *Caenorhabditis elegans*. Nature **391:**806–811.
10. **Furner, I. J., M. A. Sheikh, and C. E. Collett.** 1998. Gene silencing and homology-dependent gene silencing in *Arabidopsis*: genetic modifiers and DNA methylation. Genetics **149:**651–662.
11. **Giordano, E., R. Rendina, I. Peluso, and M. Furia.** 2002. Two-color GFP imaging demonstrates cell-autonomy of GAL4-driven RNA interference in *Drosophila*. Genetics **160:**637–648.
12. **Guimaraes, M. J., D. Peterson, A. Vicari, B. G. Cocks, N. G. Copeland, D. J. Gilbert, N. A. Jenkins, D. A. Ferrick, R. A. Kastelein, J. F. Bazan, and A. Zlotnik.** 1996. Identification of a novel selD homolog from eukaryotes, bacteria, and archaea: is there an autoregulatory mechanism in selenocysteine metabolism? Proc. Natl. Acad. Sci. USA **93:**15086–15091.
13. **Hannon, G. J.** 2002. RNA interference. Nature **418:**244–251.
14. **Hasuwa, H., K. Kaseda, T. Einarsdottir, and M. Okabe.** 2002. Small interfering RNA and gene silencing in transgenic mice and rats. FEBS Lett. **532:**227–230.
15. **Hatfield, D. L. (ed.).** 2001. Selenium: its molecular biology and role in human health. Kluwer Academic Publishers, Boston, Mass.
16. **Hatfield, D. L., and V. N. Gladyshev.** 2002. How selenium has altered our understanding of the genetic code. Mol. Cell. Biol. **22:**3565–3576.
17. **Hirosawa-Takamori, M., H. Jackle, and G. Vorbruggen.** 2000. The class 2 selenophosphate synthetase gene of *Drosophila* contains a functional mammalian-type SECIS. EMBO Rep. **1:**441–446.
18. **Ho, S. N., H. D. Hunt, R. M. Horton, J. K. Pullen, and L. R. Pease.** 1989. Site-directed mutagenesis by overlap extension using the polymerase chain reaction. Gene **77:**51–59.
19. **Kalidas, S., and D. P. Smith.** 2002. Novel genomic cDNA hybrids produce effective RNA interference in adult *Drosophila*. Neuron **33:**177–184.
20. **Kennerdell, J. R., and R. W. Carthew.** 2000. Heritable gene silencing in *Drosophila* using double-stranded RNA. Nat. Biotechnol. **18:**896–898.
21. **Kim, I. Y., M. J. Guimaraes, A. Zlotnik, J. F. Bazan, and T. C. Stadtman.** 1997. Fetal mouse selenophosphate synthetase 2 (SPS2): characterization of the cysteine mutant form overproduced in a baculovirus-insect cell system. Proc. Natl. Acad. Sci. USA **94:**418–421.
22. **Kryukov, G. V., V. M. Kryukov, and V. N. Gladyshev.** 1999. New mammalian selenocysteine-containing proteins identified with an algorithm that searches for selenocysteine insertion sequence elements. J. Biol. Chem. **274:**33888–33897.
23. **Lescure, A., D. Gautheret, P. Carbon, and A. Krol.** 1999. Novel selenoproteins identified in silico and in vivo by using a conserved RNA structural motif. J. Biol. Chem. **274:**38147–38154.
24. **Li, Y. X., M. J. Farrell, R. Liu, N. Mohanty, and M. L. Kirby.** 2000. Double-stranded RNA injection produces null phenotypes in zebrafish. Dev. Biol. **217:**394–405.
25. **Liu, Y., and D. J. Montell.** 1999. Identification of mutations that cause cell migration defects in mosaic clones. Development **126:**1869–1878.
26. **Low, S. C., J. W. Harney, and M. J. Berry.** 1995. Cloning and functional characterization of human selenophosphate synthetase, an essential component of selenoprotein synthesis. J. Biol. Chem. **270:**21659–21664.
27. **Low, S. C., and M. J. Berry.** 1996. Knowing when not to stop: selenocysteine incorporation in eukaryotes. Trends Biochem. Sci. **21:**203–208.
28. **Martin-Romero, F. J., G. V. Kryukov, A. V. Lobanov, B. A. Carlson, B. J. Lee, V. N. Gladyshev, and D. L. Hatfield.** 2001. Selenium metabolism in *Drosophila*: selenoproteins, selenoprotein mRNA expression, fertility, and mortality. J. Biol. Chem. **276:**29798–29804.
29. **Montell, C., E. Jones, E. Hafen, and G. Rubin.** 1985. Rescue of the *Drosophila* phototransduction mutation *trp* by germline transformation. Science **230:**1040–1043.
30. **Morey, M., F. Serras, and M. Corominas.** 2003. Halving the selenophosphate synthetase gene dose confers hypersensitivity to oxidative stress in *Drosophila melanogaster*. FEBS Lett. **534:**111–114.
31. **Myat, M. M., and D. J. Andrew.** 2002. Epithelial tube morphology is determined by the polarized growth and delivery of apical membrane. Cell **111:**879–891.
32. **Negeri, D., H. Eggert, R. Gienapp, and H. Saumweber.** 2002. Inducible RNA interference uncovers the *Drosophila* protein Bx42 as an essential nuclear cofactor involved in Notch signal transduction. Mech. Dev. **117:**151–162.
33. **Novoselov, S. V., M. Rao, N. V. Onoshko, H. Zhi, G. V. Kryukov, Y. Xiang, D. P. Weeks, D. L. Hatfield, and V. N. Gladyshev.** 2002. Selenoproteins and selenocysteine insertion system in the model plant cell system, *Chlamydomonas reinhardtii*. EMBO J. **21:**3681–3693.
34. **Rørth, P.** 1998. Gal4 in the *Drosophila* female germline. Mech. Dev. **78:**113–118.
35. **Seshaiah, P., B. Miller, M. M. Myat, and D. J. Andrew.** 2001. Pasilla, the *Drosophila* homologue of the human Nova-1 and Nova-2 proteins, is required for normal secretion in the salivary gland. Dev. Biol. **239:**309–322.
36. **Spradling, A. C.** 1986. P element-mediated transformation, p. 175–198. In Roberts, D. B. (ed.), *Drosophila*: a practical approach. IRL Press, Oxford, United Kingdom.
37. **Van Roessel, P., N. M. Hayward, C. S. Barros, and A. H. Brand.** 2002. Two-color GFP imaging demonstrates cell-autonomy of GAL4-driven RNA interference in *Drosophila*. Genesis **34:**170–173.
38. **Welte, M. A., S. P. Gross, M. Postner, S. M. Block, and E. F. Wieschaus.** 1998. Developmental regulation of vesicle transport in *Drosophila* embryos: forces and kinetics. Cell **92:**547–557.
39. **Wodarz, A., U. Hinz, M. Engelbert, and E. Knust.** 1995. Expression of crumbs confers apical character on plasma membrane domains of ectodermal epithelia of *Drosophila*. Cell **82:**67–76.